J|A|C|S
ARTICLES
Published on Web 12/19/2003

Experimental and Structural Evidence that Herpes 1 Kinase and Cellular DNA Polymerase(s) Discriminate on the Basis of Sugar Pucker

Victor E. Marquez,*,† Tsipi Ben-Kasus,‡ Joseph J. Barchi, Jr.,† Karen M. Green,† Marc C. Nicklaus,† and Riad Agbaria‡

Contribution from the Laboratory of Medicinal Chemistry, Center for Cancer Research, National Cancer Institute at Frederick, 376 Boyles St., Frederick, MD, 21702 and Department of Clinical Pharmacology, Faculty of Health Sciences, Ben-Gurion University of the Negev, Beer-Sheva 84105, Israel

Received August 14, 2003; E-mail: marquezv@dc37a.nci.nih.gov

Abstract: Two isomers of methanocarba (MC) thymidine (T), one an effective antiherpes agent with the pseudosugar moiety locked in the North (*N*) hemisphere of the pseudorotational cycle (**1a**, *N*-MCT) and the other an inactive isomer locked in the antipodean South (*S*) conformation (**1b**, *S*-MCT) were used to determine whether kinases and polymerases discriminate between their substrates on the basis of sugar conformation. A combined solid-state and solution conformational analysis of both compounds, coupled with the direct measurement of mono-, di-, and triphosphate levels in control cells, cells infected with the *Herpes simplex* virus, or cells transfected with the corresponding viral kinase gene (HSV-tk), suggests that kinases prefer substrates that adopt the *S* sugar conformation. On the other hand, the cellular DNA polymerase(s) of a murine tumor cell line transfected with HSV-tk incorporated almost exclusively the triphosphate of the locked *N* conformer (*N*-MCTTP), notwithstanding the presence of higher triphosphate levels of the *S*-conformer (*S*-MCTTP).

Introduction

Despite the similar structural motifs of nucleoside-based drugs consisting of a modified sugar moiety and an intact or slightly modified DNA or RNA nucleobase, the therapeutic activity of nucleoside analogues ranges from totally inactive to highly potent. In the case of 2′-deoxyribonucleoside analogues, where the desired biological response is principally derived from the incorporation of the drug into DNA, the final outcome is determined by the ability of the molecule to interact effectively with several different classes of enzymes: the three activating kinases and the final target, DNA polymerase. To probe the conformational preferences of these enzymes for their nucleoside(-tide) substrates, and to ascertain whether a particular conformational preference is a factor in determining biological activity, we have used 2′-deoxyribonucleoside analogues built on a rigid bicyclo[3.1.0]hexane scaffold to effectively lock the conformation of the pseudosugar moiety into one of the two rapidly equilibrating North (*N*) and South (*S*) conformations that normally characterize the sugar moiety of standard nucleosides.

An unrestricted furanose ring normally adopts a number of conformations that can be conveniently described by the value of *P* in the pseudorotational cycle (Figure 1).[1] The value of *P* depends on the five endocyclic sugar torsion angles ($\nu_0 - \nu_4$) of the furanose ring. By convention, a phase angle $P = 0°$ corresponds to a perfect *N* conformation possessing a symmetrical twist form $^3T_2$, whereas the absolute *S* antipode, $_3T^2$, is represented by $P = 180°$ (Figure 1). A close inspection of the available crystallographic data for individual nucleosides and nucleotides reveals that the puckering modes of the furanose

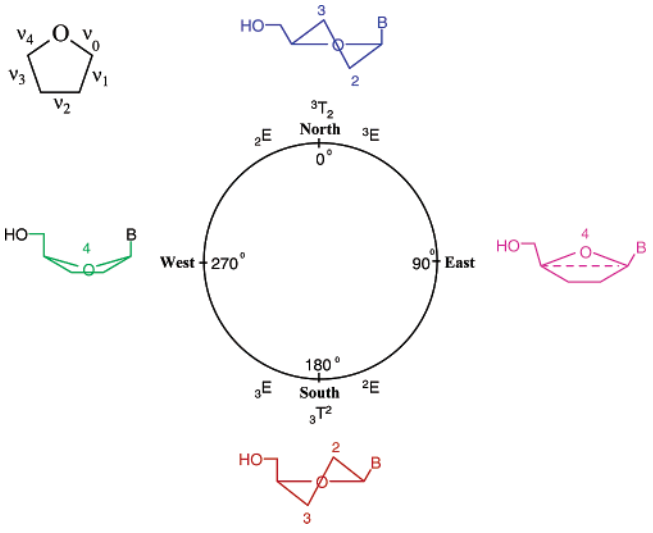

Figure 1. Pseudorotation cycle of the furanose ring in nucleosides. The populated ranges of *N* and *S* conformations are highlighted.

† Laboratory of Medicinal Chemistry, Center for Cancer Research, National Cancer Institute at Frederick.

‡ Department of Clinical Pharmacology, Faculty of Health Sciences, Ben-Gurion University of the Negev.

(1) Altona, C.; Sundaralingam, M. *J. Am. Chem. Soc.* **1972**, *94*, 8205−8212.

ring cluster in two antipodal domains around a 3′-*endo* (^{3}E, *N*) and a 2′-*endo* (^{2}E, *S*) envelope (E) conformations.[2] However, in solution, the sugar puckering fluctuates rapidly between these two conformational extremes. In the *N* conformation, *P* values are found in a range between 342° (−18°) and 18° [$_2$E → $^3T_2$ → ^{3}E (3′-*endo*)], whereas in the antipodal *S* conformation the range is between 162° and 198° [^{2}E (2′-*endo*) → $_3T^2$ → $_3$E].[1]

When the sugar rings occupy similar domains of *P* in polymeric structures (e.g., DNA and RNA) it leads to two different categories of polynucleotide conformations, known as A- and B-type families.[3] The 3′-*endo* conformation is typical of the A-type families and the 2′-*endo* is characteristic of the B-type families. In reference to their position in the pseudorotational cycle, these preferred sugar puckerings (3′-*endo* and 2′-*endo*) are also generically described, respectively, as North (*N*) and South (*S*) conformations.[3] The transition between *N* and *S* antipodes corresponds to an inversion of ring puckering that is accompanied by changes in the axial and equatorial disposition of all of the substituents on the sugar ring. In polynucleotides, these differences affect the distance between adjacent phosphates, and, as a consequence, the helical arrangements of A- and B-type families are distinctly different.[3] Changes between A- and B-type families can occur in response to environmental factors, such as degree of hydration, salt concentration, metal ion coordination, protein binding, and interactions with small molecules, all of which affect biological function.[4]

Because individual nucleosides and nucleotides can crystallize with the ribose or 2′-deoxyribose rings in either a *N* or *S* conformation, and in solution these conformations show a rapid dynamic equilibrium, it can be concluded that the ribose ring has little preference for either state. Indeed, the energy barrier for interconversion between the *N* and *S* states is quite low.[5] However, when the same *N* ⇔ *S* change occurs within a polymeric structure, the energy differences between the resulting A and B structures—which depend on the balance of forces that include electrostatics, van der Waals interactions, torsional flexibility, entropies of counterions and solvation—are magnified.[6]

In an alternative situation when a single nucleoside(-tide) binds to an organized macromolecule (i.e. an enzyme), it is expected that the architecture of the binding pocket will impose a specific conformational demand on the sugar ring (*N* or *S*) for optimal fit that should result in measurable differences in terms of energy of binding and/or catalytic activity. The question we wish to address in the present work is whether the stability and catalytic efficiency of these complexes changes as a function of the conformation of the sugar moiety.

Conformationally rigid nucleosides built on a bicyclo[3.1.0]-hexane template can lock the embedded cyclopentane ring into an envelope conformation ($_2$E, *P* = 342°) at the extreme edge

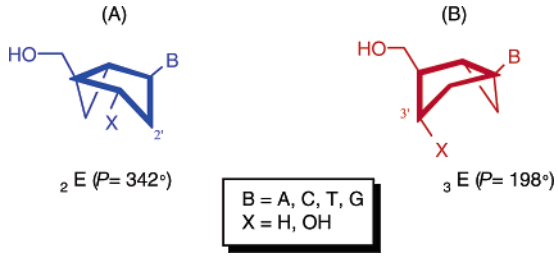

Figure 2. Conformationally locked *N* (A) and *S* (B) bicyclo[3.1.0]hexane nucleosides.

of the typical range for *N* conformers (*P* = 0° ± 18°) (Figure 2A).[7−10] Changing the disposition of the fused three-member ring relative to the position of the nucleobase engenders a similarly locked *S* conformation (Figure 2B).[11−14] This conformation also resides at the extreme edge of the range populated by typical nucleosides in the *S* domain ($_3$E, *P* = 198°). Using this type of conformationally locked nucleosides, we have already determined the conformational preferences of a number of enzymes including adenosine deaminase (ADA),[13] HIV reverse transcriptase,[15] DNA (cytosine-C5) methyl transferase,[16] and several subtypes of adenosine receptors.[17−20]

The conformationally locked antipodes of thymidine that are the main subject of this paper, *N*-methanocarbathymidine (*N*-MCT, **1a**) and *S*-methanocarbathymidine (*S*-MCT, **1b**) provide yet another example of clear conformational discrimination: only the *N* antipode displays activity against *herpes simplex* virus types 1 and 2 (HSV-1/2).[9,21] In this particular case, however, the problem in attempting to correlate a conformational preference with a specific activity is that the final biological outcome depends on the ability of the compound to interact effectively with several different classes of enzymes: the three activating kinases and the final target, DNA polymerase. Herein, we demonstrate that the success or failure of these locked analogues as drugs correlates directly with the antipodal conformational preferences of the herpes thymidine kinase (HSV-tk) and the cellular DNA polymerase(s).

(2) de Leeuw, H. P. M.; Haasnoot, C. A. G.; Altona, C. *Isr. J. Chem.* **1980**, *20*, 108−126.
(3) Saenger, W. *Principles in Nucleic Acid Structure*; Springer-Verlag: New York, Berlin, Heilderberg, 1984. Chapter 9.
(4) Neidle, S. *Nucleic Acid Structure and Recognition*; Oxford University Press: 2002. Chapter 5.
(5) ref 3, Chapter 4.
(6) Jayaram, B.; Sprous, D.; Young, M. A.; Beveridge, D. L. *J. Am. Chem. Soc.* **1998**, *120*, 10 629−10 633.
(7) Rodriguez, J. B.; Marquez, V. E.; Nicklaus, M. C.; Barchi, Jr., J. J. *Tetrahedron Lett.* **1993**, *34*, 6233−6236.
(8) Rodriguez, J. B.; Marquez, V. E.; Nicklaus, M. C.; Mitsuya, H.; Barchi Jr., J. J. *J. Med. Chem.* **1994**, *37*, 3389−3399.
(9) Marquez, V. E.; Siddiqui, M. A.; Ezzitouni, A.; Russ, P.; Wang, J. Y.; Wagner, R. W.; Matteucci, M. D. *J. Med. Chem.* **1996**, *39*, 3739−3747.
(10) Siddiqui, M. A.; Ford, Jr. H.; George, C.; Marquez, V. E. *Nucleosides Nucleotides* **1996**, *15*, 235−250.
(11) Ezzitouni, A.; Barchi Jr., J. J.; Marquez, V. E. *J. Chem. Soc., Chem. Commun.* **1995**, 1345−1346.
(12) Ezzitouni, A.; Marquez, V. E. *J. Chem. Soc., Perkin Trans 1* **1997**, 1073−1078.
(13) Marquez. V. E.; Russ, P.; Alonso, R.; Siddiqui, M. A.; Hernandez, S.; George, C.; Nicklaus, M. C.; Dai, F.; Ford, Jr., H. *Helv. Chim. Acta* **1999**, *82*, 2119−2129.
(14) Shin, K. J.; Moon, H. R.; George, C.; Marquez, V. E. *J. Org. Chem.* **2000**, *65*, 2172−2178.
(15) Marquez, V. E.; Ezzitouni, A.; Russ, P.; Siddiqui, M. A.; Ford Jr., H.; Feldman, R. J.; Mitsuya, H.; George, C.; Barchi Jr., J. J. *J. Am. Chem. Soc.* **1998**, *120*, 2780−2789.
(16) Wang, P.; Bransk, A. S.; Banavali, N. K.; Nicklaus, M. C.; Marquez, V. E.; Christman, J. K.; MacKerell, A. D. *J. Am. Chem. Soc.* **2000**, *122*, 12 422−12 434.
(17) Jacobson, K. A.; Ji, X. D.; Li, A.; Melman, N.; Siddiqui, M. A.; Shin, K. J.; Marquez, V. E.; Ravi, R. G. *J. Med. Chem.* **2000**, *43*, 2196−2203.
(18) Lee, K.; Ravi, R.; Ji, X. D.; Marquez, V. E. *Bioorg. Med. Chem. Lett.* **2001**, *11*, 1333−1337.
(19) Ravi, G.; Lee, K.; Ji, X. D.; Kim, H. S.; Soltysiak, K. A.; Marquez, V. E.; Jacobson, K. A. *Bioorg. Med. Chem. Lett.* **2001**, *11*, 2295−2300.
(20) Kim, H. S.; Ravi, R. G.; Marquez, V. E.; Maddileti, S.; Whilborg, A.-K.; Erlinge, D.; Malsmjo, M.; Boyer, J. L.; Harden, T. K.; Jacobson, K. A. *J. Med. Chem.* **2002**, *45*, 208−218.
(21) Zalah, L.; Huleihel, M.; Manor, E.; Konson, A.; Ford Jr., H.; Marquez, V. E.; Johns, D. G.; Agbaria R. *Antiviral Res.* **2002**, *55*, 63−75.

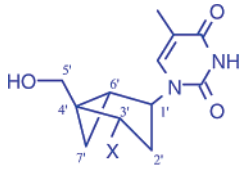

1a, X = OH
2a, X = N 3

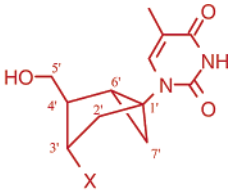

1b, X = OH
2b, X = N 3

Results and Discussion

NMR and Solid-State Conformational Analysis of the Substrates. a. The Conformation of the Pseudosugar Moiety. We showed previously, using NMR-based structural analysis, that the pseudoboat disposition of the bicyclo[3.1.0]hexane system in the AZT analogues **2a** [*N*-methanocarba -AZT] and **2b** [*S*-methanocarba -AZT] was maintained by the molecule in solution, even at high temperature, and that it faithfully mirrored the conformation in the solid state.[15] Similar results for the *N*- and *S*-MCT derivatives (**1a** and **1b**) used in the present study confirmed a similar pseudoboat conformation: dihedral angles H1′−C1′−C2′−H2β′ and H1′−C1′−C6′−H6′ in compound **1a**, and H4′−C4′−C6′−H6′ and H3′−C3′−C2′−H2′α in compound **1b**, are close to 90° with the corresponding *J* coupling constants approaching zero.[9,12]

b. The Conformation of the Base. Although the sugar pucker is the main conformational determinant in a nucleoside, an important associated parameter is the glycosyl torsion angle χ whose value determines the syn or anti disposition of the base relative to the sugar moiety. Generally, χ tends to be anti when the sugar pucker is *N* and syn when the sugar pucker is *S*.[22] The crystal structures of **1a**,[23] **1b**,[24] **2a**[15] and **2b**[15] confirmed that χ responded equivalently in bicyclo[3.1.0]hexane nucleosides: **1a** and **2a** (both *N*) display the pyrimidine base in the anti range and **1b** and **2b** (both *S*) display the pyrimidine ring in the syn range. Our conformational analysis also revealed a similar *N*-anti/*S*-syn correlation after computationally sampling the entire conformational space of χ from 0° to 360° (Figure 3). For *N*-MCT (**1a**), an energy barrier of ca. 10 kcal/mol separates the most stable anti conformation ($\chi = -150°$) from the less stable syn conformation ($\chi = 90°$). In the case of *S*-MCT, the most stable syn conformation ($\chi = 60°$) is separated from the less stable anti conformation ($\chi = -120°$) by a higher energy barrier of 15 kcal/mol. In both cases, the integrity of the bicyclo[3.1.0]hexane system remained constant during the calculations as indicated by the small variance of *P* across the entire range of χ (data not shown).

In solution, the NMR data in $CDCl_3$ for AZT analogues **2a** and **2b** also mirrored the crystal data with respect to χ, i.e., the *N* analogue (**2a)** favored the anti range, while the *S* analogue (**2b**) favored the syn range.[15] The results for *N*-MCT and *S*-MCT were similar in $CDCl_3$. However, when the solvent was D_2O, whereas the base disposition in the *N* analogue (**1a)** remained anti, that of the *S* analogue **1b** switched from syn to anti indicating the existence of a syn ⇔ anti equilibrium in this solvent (Figure 4). The anti disposition was easily diagnosed

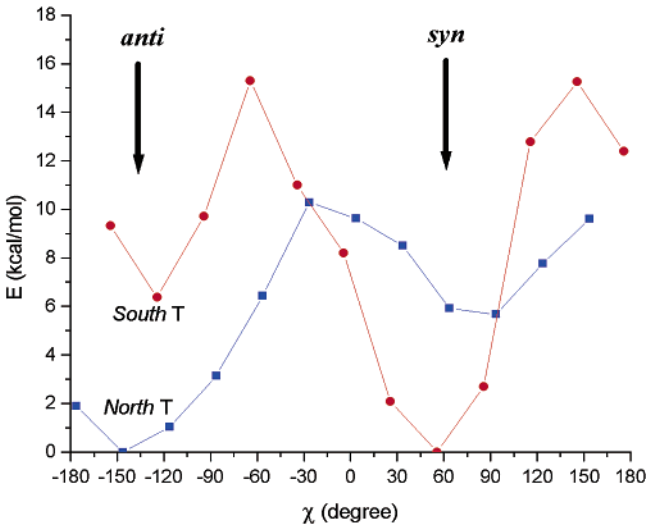

Figure 3. Plots of energy as a function of χ for ab initio-optimized structures of *N*-MCT (blue) and *S*-MCT (red). Computations performed for vacuum environment.

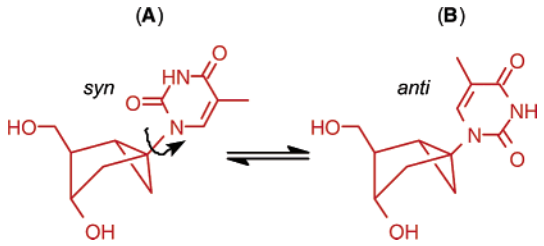

Figure 4. Syn-anti equilibrium in *S*-MCT (**1b**): The conformation is syn (A) when the C2 carbonyl of the base lies over the sugar ring and anti (B) when its disposition is away from the sugar in the opposite direction.

by the strong NOE interactions between the H6 proton of the base and the protons on the methylene CH_2OH group (arrows in Figure 5A,B), whereas the syn disposition displayed no NOE interactions between the same set of protons (Figure 5C). In the solid state, and possibly in a nonaqueous environment (i.e., $CHCl_3$), the *S* analogues (**1b** and **2b**) show a strong H-bond between the CH_2OH and the O2 carbonyl oxygen of the pyrimidine, which is responsible for maintaining the base in the syn orientation. Formation of this H-bond was also supported by the calculations shown in Figure 3, which were performed in a vacuum environment. In an aqueous solution, however, this H-bond probably weakens due to competition by water molecules, permitting more torsional freedom of the glycosyl torsion angle χ, allowing the base to sample the anti range. Esterification of the CH_2OH of the *S* analogue (**1b**) as the monophosphate also forced χ into the anti range (data not shown) as no intramolecular H-bond is possible.

The results above confirmed that the correlation between χ and sugar pucker for bicyclo[3.1.0]hexane nucleosides is identical to that observed in conventional nucleosides and that χ responds accordingly to changes in either sugar puckering or the environment. For this reason, our querying of HSV-tk and the cellular DNA polymerase(s) for a specific conformational preference will be correlated primarily with sugar pucker since the torsion angle χ can usually adopt a wider range of energetically favorable dispositions.[25]

(22) ref 3, Chapter 2.
(23) Altmann, K. H.; Kesselring, R.; Francotte, E.; Rihs, G. *Tetrahedron Lett.* **1994**, *35*, 2331−2334.
(24) Altmann, K. H.; Imwinkelried, R.; Kesselring, R.; Rihs, G. *Tetrahedron Lett.* **1994**, *35*, 7625−7628.
(25) Marquez, V. E.; Russ, P.; Alonso, R.; Siddiqui, M. A.; Shin, K. J.; George, C.; Nicklaus, M. C.; Dai, F.; Ford Jr., H. *Nucleosides Nucleotides* **1999**, *18*, 521−530.

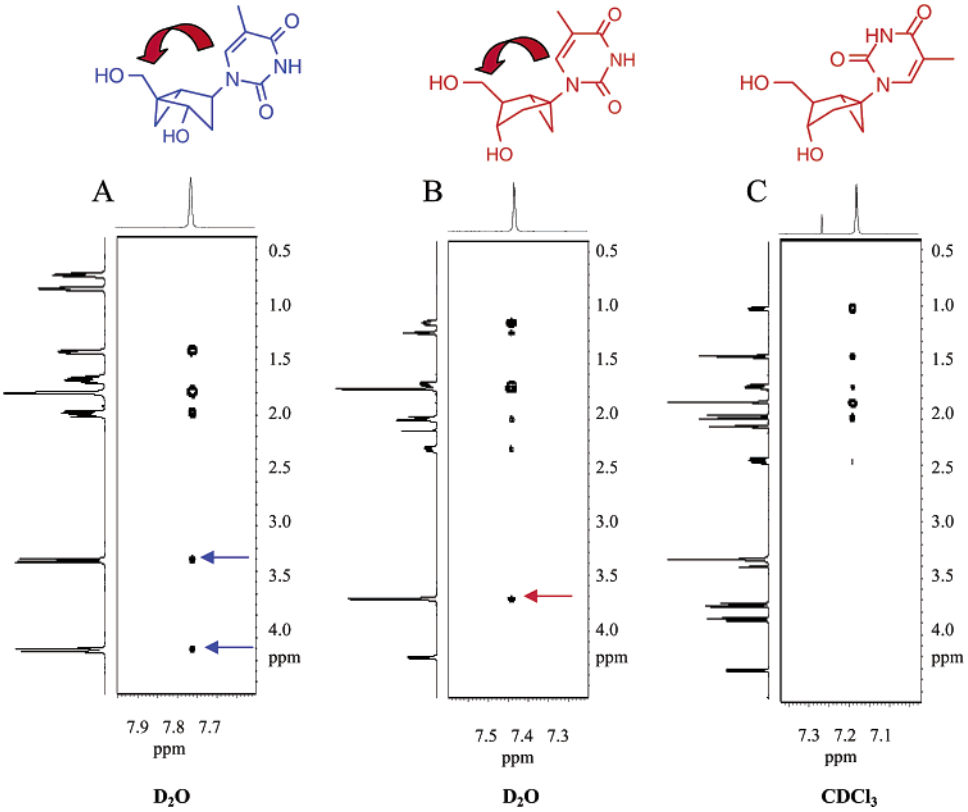

Figure 5. Expanded NOESY spectra (300 ms mix) of compounds **1a** (A) and **1b** (B) in D_2O, and compound **1a** (C) in $CDCl_3$ showing correlations to the H6 proton of the thymine base (F2, horizontal axis) with the protons on the bicyclo[3.1.0]hexane system (F1, vertical axis). The χ angle about the pseudoanomeric position is in the anti range in D_2O (A and B) and in the syn range in $CDCl_3$ (C) determined by the presence or absence of NOEs (arrows) to the side chain CH_2OH protons. For compound **1a** (A), these protons resonate at distinct chemical shifts (4.1 and 3.4 ppm) whereas for **1b** (B) they are degenerate and resonate as a 2-proton doublet (3.6 ppm). In $CDCl_3$ (C) the same protons for **1b** appear as separate AB multiplets of the H4′−H5′−H5″ ABX system (3.6 and 3.7 ppm). The singlet at 7.25 in the F2 dimension in (C) is residual $CHCl_3$.

Interaction of *N*-MCT (1a) and *S*-MCT (1b) with HSV-tk. As with the well-known antiherpes compounds ganciclovir (GCV) and acyclovir (ACV), the antiviral activity of *N*-MCT (**1a**) and *S*-MCT (**1a**) has to depend on the effective phosphorylation catalyzed by the herpes thymidine kinase (HSV-tk). This enzyme initially phosphorylates the drugs providing the substrate for the cellular kinases to complete the pathway leading to the triphosphate metabolites. These, in turn, are the final substrates intended to interact with cellular DNA polymerases to block DNA synthesis and/or DNA function. We have already demonstrated that the antiviral activity of *N*-MCT (**1a**) against HSV-1 is similar to that of ACV and GCV, and that its activity is indeed mediated by the triphosphate metabolite.[21] The conformationally locked antipode, *S*-MCT (**1b**), on the other hand, was devoid of antiherpes activity,[9] which could result from either the inability of the herpes kinase to phosphorylate *S*-MCT, or the failure of the DNA polymerase to efficiently incorporate the corresponding triphosphate of *S*-MCT. To address these questions, studies were performed using radiolabeled substrates.

Uninfected and HSV-1 infected Vero cells were separately incubated with [methyl-^{3}H]-*N*-MCT or [methyl-^{3}H]-*S*-MCT (10 μM, 5 μCi/ml) for 6 h. The cells were harvested and the methanol extracts were analyzed by SAX-HPLC (Table 1, Figure 6). The results showed that in infected cells, phosphate levels of *S*-MCT nucleotides were higher than those of achieved with *N*-MCT, particularly for the di- and tri-phosphates, with South/North (*S*/*N*) phosphorylation ratios of ca. 0.9, 4.6, and 2.5 for the mono-, di-, and triphosphates, respectively. The identity of the metabolites was confirmed by HPLC after alkaline phosphatase or venom phosphodiesterase treatment, and by comparison with authentic standards (data not shown). A low level of *N*-MCT-monophosphate (*N*-MCT-MP) was also detected in uninfected cells, but *S*-MCT-MP was essentially undetectable in uninfected cells. This means that *N*-MCT is a weak substrate for cellular thymidine kinase, but the rest of the cellular machinery is unable to convert the monophosphate to the diphosphate and beyond, suggesting that a second phorphorylation step must have been catalyzed by HSV-tk to activate the drug. This result is in keeping with the known role of HSV-tk as a dTMP phosphorylating enzyme.[21]

Consistent with the role of HSV-tk as the activating enzyme, exponentially growing MC38 tumor cells transfected with the kinase (MC38/*HSV-tk*) and incubated with [methyl-^{3}H]-*N*-MCT or [methyl-^{3}H]-*S*-MCT (10 μM, 5 μCi/ml) showed efficient formation of phosphate metabolites. The results were similar to those with Vero cells infected with HSV-1, except that the

Table 1. Levels of *N*-MCT and *S*-MCT Phosphates (pmoles/10^6 cells) in Uninfected and HSV-1-infected Vero Cells

	N-MCT		*S*-MCT	
metabolite	uninfected cells	HSV-1 infected	uninfected cells	HSV-1 infected
MP	3.212 ± 0.152	76 ± 0.9	0.031 ± 0.034	72 ± 5.4
DP	0.032 ± 0.024	82 ± 6.3	0.021 ± 0.021	378 ± 29
TP	0.019 ± 0.012	197 ± 14.6	0.028 ± 0.011	490 ± 67

MP = monophosphate; DP = diphosphate; TP = triphosphate. [a] Assessment of phosphorylation in whole cells.

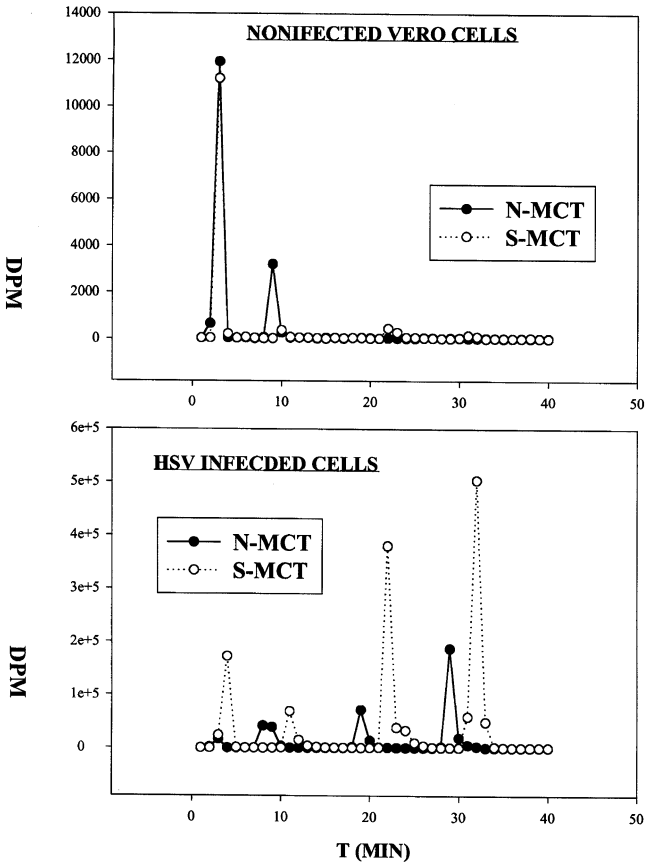

Figure 6. Phosporylation of *N*-MCT (**1a**) and *S*-MCT (**1b**) in noninfected (A) and HSV-1-infected (B) Vero cells.

S/*N* ratios of mono-, di- and tri-phosphates were lower: 0.3, 1.57, and 1.32, respectively (data not shown). As was seen in Vero cells, despite the higher levels of *S*-MCT phosphate metabolites produced in the MC38/HSV-tk cells, particularly *S*-MCT-TP, *S*-MCT had only a modest effect in inhibiting cell growth (30% inhibition at 10 μM). This is in sharp contrast to *N*-MCT, which was reported to have an IC_{50} of 2.9 μM in MC38/*HSV-tk* cells.[26] The results from these experiments support the concept that HSV-tk has a definitive preference for the *S* conformer in controlling the second phosphorylation step. Similarly, judging from the levels of the triphosphate metabolites, it would appear that the cellular dinucleotide kinase also prefers the *S* conformer. Concerning the first phosphorylation step, the fact that *N*-MCT appears to be a weak substrate for the cytoplasmic thymidine kinase (tk1), whereas *S*-MCT is not a substrate at all, seems to contradict our hypothesis at first glance. We surmise that tk1, which is the kinase with the most restrictive substrate specificity, is able to detect the preferred syn disposition of *S*-MCT, and thus fails to recognize it as a substrate. In the case of *N*-MCT, although the sugar pucker is not optimal, the predominant rotamer is anti, as in the natural tk1 substrates thymidine and deoxyuridine. Even the less discriminating HSV-tk appears to recognize the same conformational bias of χ in *S*-MCT, resulting in lower *S*/*N* ratios for the first phosphorylation step. However, once the syn/anti energy barrier for the first sluggish phosphorylation step is surmounted, the value of χ will remain entirely anti, beginning with the monophosphate (vide supra) after which the *S*-puckered substrates become preferentially phosphorylated.

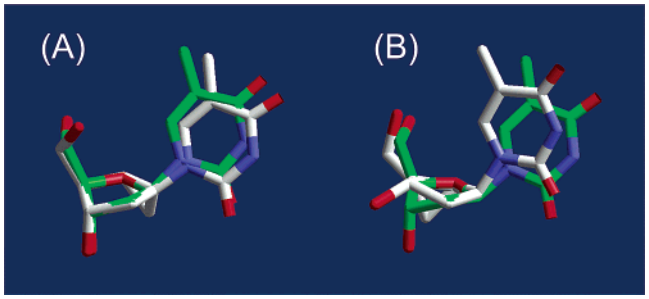

Figure 7. (A) Superposition of thymidine (green) and *S*-MCT (white). (B) Superposition of thymidine (green) and *N*-MCT (white). The flexible sugar moiety of thymidine adopts the *S* conformation superposable on the restricted conformation of *S*-MCT in (A).

b. Conformational Analysis. A comparison of the structures of the locked conformers of *N*-MCT and *S*-MCT with the crystal structure of the natural substrate thymidine[27] shows quite clearly that the locked cyclopentane ring embedded into the bicyclo-[3.1.0]hexane pesudosugar of *S*-MCT mimics perfectly the contour of the sugar ring of thymidine (Figure 7A), while the cyclopentane ring of *N*-MCT does not (Figure 7B). A critically differentiating feature is the contrasting axial versus equatorial orientation of the 3′-OH group, which in the case of the normal substrate thymidine forms a well-defined network of H-bonds with Tyr101 and Glu225 at the active site.[28,29] In agreement with this analysis, the published structure of the HSV1-tk:*N*-MCT complex shows a poorer fit of the substrate at the active site with the 3′-OH group of the pseudosugar moiety displaced 3.7 Å away from Glu225 and 4.1 Å away from Tyr101[OH], indicating a lack of direct of H-bonding with these amino acids.[30]

Incorporation of *N*-MCT-Triphosphate and *S*-MCT-Triphosphate into DNA. Despite the efficient phosphorylation of *S*-MCT, the compound was devoid of antiviral activity against HSV-1[9] and antitumor activity in MC38/*HSV-tk* transduced cells (vide supra). This suggested that the inactivity of the compound could perhaps be caused failure of the cellular DNA polymerase to incorporate *S*-MCT-triphosphate. Examination of DNA extracts from tumor cells [MC38 (wild-type) and MC38/*HSV-tk*] after a 24-h exposure to radiolabeled [methyl-^{3}H]-*N*-MCT and [methyl-^{3}H]-*S*-MCT (10 μM; 10 μCi/ml) showed that wild-type MC38 cells incorporated negligible amounts of both *N*- or *S*-MCT into DNA. On the other hand, the *HSV-tk*-transduced cells incorporated significant quantities of *N*-MCT at a level even higher than for GCV (Figure 8). The negligible amounts of *S*-MCT incorporated implies that the host DNA polymerase(s) may prefer incorporating nucleotide triphosphate substrates with an *N* sugar pucker, effectively discriminating against the antipodal *S* conformer despite the presence of higher levels of the *S* triphosphate metabolite in the cell. This result is also consistent with our previous observation that *N*-methanocarba-

(26) Noy, R.; Ben-Zvi, Z.; Elezra, M.; Candoti, F.; Ford Jr., H.; Morris, J. C.; Marquez, V. E.; Johns, D. G.; Agbaria, R. *Mol. Cancer Chemother*. **2002**, *1*, 585−593.
(27) Young, D. W.; Tollin, P.; Wilson, H. R. *Acta Crystallogr., Sect. B*, **1969**, *25*, 1423−1432.
(28) Wild, K.; Bohner, T.; Folkers, G.; Schulz, G. E. *Protein Sci*. **1997**, *6*, 2097−2106.
(29) Champness, J. N.; Bennett, M. S.; Wien, F.; Visse, R.; Summers, W. C.; Herdewijn, P.; De Clercq, E.; Ostrowski, T.; Jarvest, R. L.; Sanderson, M. R. *Proteins* **1998**, *32*, 350−361.
(30) Prota, A.; Vogt, J.; Pilger, B.; Perozzo, R.; Wurth, C.; Marquez, V. E.; Russ, P.; Schultz, G. E.; Folkers, G.; Scapozza, L. *Biochemistry* **2000**, *39*, 9597−9603.

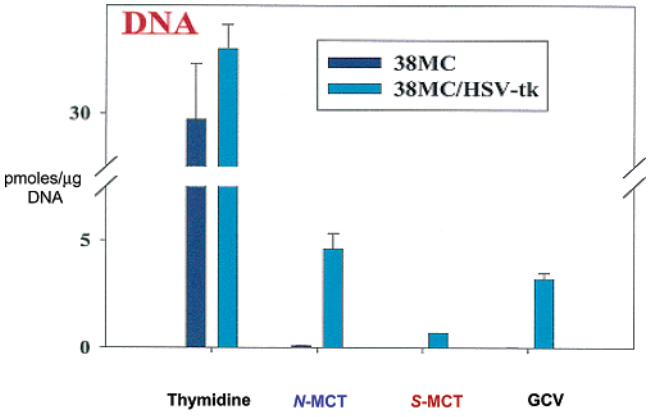

Figure 8. DNA incorporation of Thymidine, *S*-MCT, *N*-MCT and GCV in murine MC38 cells before and after HSV-tk transfection.

AZT-triphosphate was more effective in inhibiting HIV reverse transcriptase than *S*-AZT-triphosphate.[15]

Concluding Remarks

In nucleoside biosynthesis, the salvage pathway complements the *de novo* pathway by providing cells with deoxyribonucleotide precursors for DNA synthesis and repair. Thymidine kinase (tk1) is a key enzyme in the pyrimidine salvage pathway, catalyzing the phosphorylation of thymidine. Although human tk1 has significant substrate specificity, the *herpes simplex* virus type 1 kinase (*HSV-tk*) can phosphorylate a broad range of nucleoside analogues, activating these analogues exclusively in virally infected cells. When a nucleoside analogue is converted to the triphosphate, following the initial activation by *HSV-tk*, its capacity to function as substrate for the DNA polymerase(s) will determine the final therapeutic outcome.

The principal objective of this work was to ask whether these different classes of enzymes, the activating kinases and the DNA polymerases, select their substrates on the basis of the conformational preferences of the individual nucleosides or nucleotides. The conclusion that cellular DNA polymerases and *HSV-tk* have contrasting conformational preferences for *N*-MCT (**1a**) versus *S*-MCT (**1b**) can be explained on structural grounds. During phosphorylation, the 5′-position bearing the OH, or phosphate group, needs to be accessible. This is easily accomplished if the sugar adopts the *S* conformation that favors the less encumbered *ap* disposition for the torsion angle γ. In addition, in the *S* conformation there will be less interference between the 5′-OH and 3′-OH because these groups are approximately 7 Å apart rather than 5.9 Å as they are in the *N* conformation.[3] A direct comparison between structures **1a** and **1b** shows clearly that there is a nearly perfect fit for *S*-MCT with the substrate thymidine, while the fit for the antipodal *N*-MCT is less than optimal. Although we do not have a full set of crystal structures to explain the polymerase's choice for *N*-MCT over *S*-MCT, the conformational preference for *N*-MCT is in keeping with the polymerase's predilection for constraining the nascent template-primer duplex in the A-form (*N*-sugars).[31] Indeed, current models based on crystallographic analysis suggest that the intrinsic fidelity of a polymerase depends to some extent on its ability to impose an A-conformation which provides a structural buffer to conformational variability.[32] In contrast, polymerase β which binds to a B-DNA duplex is the most inaccurate DNA polymerase.[32] It has also been proposed that the more anhydrous A-conformation at the polymerase active site may contribute to polymerase fidelity by minimizing mismatches.[31−33] The possibility that the different conformational preferences between kinases and polymerases would result from evolutionary forces acting to achieve optimal catalytic efficiency by binding to a nucleoside(-tide) with a specific sugar conformation is an attractive idea, but goes beyond the scope of this study.

This work provides the first example of locked nucleoside analogues built on a bicyclo[3.1.0]hexane template being successfully used as substrates to track enzymes' conformational preferences through the sequence of the triad of anabolic kinases (i.e., *HSV-tk* for the first two steps and cellular kinases for the final step) and DNA polymerase(s). Although the results are limited to cells infected with the herpes virus, or transfected with the *HSV-tk* gene, one can speculate, based on structural grounds, that other nucleoside(-tide) kinases may show a similar penchant of phosphorylating substrates displaying the *S*-conformation. This, and the contrasting conformational preference of the cellular DNA polymerase for the locked *N*-substrate, shows how important the flexibility of the ribose ring is for its capacity to adapt to the conformational demands of each of the enzymes. The opposing preferences of kinases and polymerases revealed with the help of these locked nucleosides suggest that even minor changes in the patterns of substitutions on the sugar and nucleobase moieties of "conventional" nucleoside drugs can alter the *N*/*S* equilibrium and thereby profoundly impact the recognition of the compound as a substrate at every step. These locked nucleosides also have the potential to provide compounds that preclude an undesirable event, such as the incorporation into DNA in cases where the main biological targets are enzymes involved in de novo or salvage pathways of nucleoside-(-tide) biosynthesis.

Experimental Procedures

Preparation of Cell Extract for Metabolite Analysis. Vero cell cultures (4×10^6/25 mL flask) were infected with 1 PFU/cell of HSV-1. After a 2 h incubation period, the cells were incubated with radioactive [Me-^{3}H]-*N*-MCT or [Me-^{3}H]-*S*-MCT, 10 μM, 5 μCi/ml. These compounds were purchased from Moravek Biochemicals, Brea, CA [specific activities of 1100 and 1250 dpm/pmol for [Me-^{3}H]-*N*-MCT and [Me-^{3}H]-*S*-MCT, respectively]. As a control, uninfected cells were treated with the radioactive drugs. At the end of a 6 h incubation period, cells were washed three times with PBS, trypsinized and recovered by centrifugation. The dry pellets were suspended in 250 μL of 60% methanol (HPLC grade), and heated at 95 °C for 3 min. After centrifugation at 12 000 × *g* for 10 min, the clear supernatant fractions were evaporated under nitrogen and redissolved in 250 μL of water. Aliquots of this solution were analyzed by anion-exchanged (SAX-10) HPLC.

HPLC Separation of Metabolites. The separation of [Me-^{3}H]-*N*-MCT, [Me-^{3}H]-*S*-MCT and their phosphorylated metabolites was carried out using a Hewlett-Packard 1100 HPLC with a diode-array UV absorption detector. A Partisil-10 SAX column (250 × 4.6 mm) was used with the following elution program: 0−5 min, 100% buffer A (0.01 M ammonium phosphate, native pH); 5−20 min, linear gradient to 25% buffer B (0.7 M ammonium phosphate with 10% methanol); 20−30 min, linear gradient to 100% buffer B; 30−40 min 100% buffer B; 40−55 min, linear gradient to 100% buffer A and equilibration.

(31) Timsit, Y. *J. Biomol. Struct. Dyn.* **2000**, 169−176, Sp. Iss. S1.
(32) Timsit, Y. *J. Mol. Biol.* **1999**, *293*, 835−853.
(33) Mayer, C.; Timsit, Y. *Cell Mol. Biol.* **2001**, *47*, 815−522.

The flow rate was 2 mL/min. One minute fractions were collected and radioactivity was measured by scintillation spectrometry. The retention times were as follows: *N*-MCT (3 min), *N*-MCT-monophosphate (9 min), *N*-MCT-diphosphate (19 min), and *N*-MCT-triphosphate (29 min); *S*-MCT (4 min), *S*-MCT-monophosphate (11 min), *S*-MCT-diphosphate (22 min), and *S*-MCT-triphosphate (31 min). Fractions containing radiolabeled drugs were quantitated based on the known specific activity of the parent tritiated compounds.

Incorporation of *N*-MCT and *S*-MCT into DNA. DNA was isolated using the TRI reagent procedure. Briefly, 50×10^6 cells were incubated for 24 h with either *N*-MCT or *S*-MCT (10 μM; 10 μCi/ml); at the end of the incubation, cells were washed three times with cold PBS, harvested by trypsinization, and collected by centrifugation. One mL of TRI reagent (guanidine thiocyanate and phenol in a monophasic solution) was added to the cell pellet, solubilizing the DNA, RNA, and protein. Chloroform was then added, and the mixture was centrifuged. RNA (in the aqueous phase) and DNA (in the interphase) were then separated and quantified according to the TRI reagent protocol.

NMR Experiments. NMR spectra for characterization purposes were collected on a Varian spectrometer with a three channel INOVA console at 500 MHz using an inverse detection triple resonance probe with an actively shielded *Z*-axis gradient (IDTG, Nalorac corp., Martinez, CA.). One-dimensional (1-D) ^{1}H spectra were collected with 32k complex points and zero-filled to 64 K. Resolution enhancement with a Gaussian function was performed prior to Fourier transformation. Coupling constants were read from these resolution-enhanced 1-D spectra for first-order multiplets. Gradient-enhanced COSY spectra were acquired with encoding and decoding gradients prior to and after the second 90° pulse. NOESY spectra were obtained using standard pulse sequences (Varian pulse sequence NOESY from the CHEMPACK suite of programs, provided by Krish Krishnamurthy, present address Eli Lilly and Company, Indianapolis, IN) in both D_2O and $CDCl_3$ solution with a mixing time of 300 ms. For these spectra, 16 or 32 transients were collected for each of 200 increments in F1. The data were processed with Gaussian apodizations in each dimension and backward linear prediction was applied in F1 followed by DC corrections. Data obtained in the 2-dimensional NOESY experiments were further confirmed by collecting selective 1-Dimensional NOE spectra using the method of Shaka[34] (Varian pulse sequence NOESY1D from the CHEMPACK) employing a homospoil gradient pulse for randomization of magnetization prior to the relaxation delay. Sech180 shaped pulses were used for selective excitation of specific resonances. For 1D-NOE experiments, 128 transients/irradiation were collected, and the FIDs were Fourier transformed using no apodization or special processing functions. The probehead temperature was maintained at 25 °C for all experiments and no attempt was made to deoxygenate the samples.

Molecular Modeling. The X-ray structures of **1a** (LETJEZ)[23] and **1b (**YESMIS)[24] were taken from the Cambridge Structural Database and imported into the molecular modeling program QUANTA (MSI, Inc., now Accelrys Corp.) and the missing hydrogen atoms were added. Following energy minimization using QUANTA's molecular mechanics program CHARMm, the structures were pre-optimized at the ab initio level using the program Spartan (Wavefunction, Inc.) at the HF/3-21G* level of theory. These pre-optimized geometries were re-optimized using the Density Functional Theory (DFT) method in the program Gaussian 94, revision D.3 (Gaussian, Inc.) at the B3LYP/6-31G(d) level of theory. These structures, which were assumed to be local or global energy minima, were then explored in a potential energy scan (PES) of the dihedral angle χ by rotating the base in angle steps of 30°. Each of the resulting geometries was optimized for all internal coordinates, except χ, using the Gaussian DFT method at the same B3LYP/6−31(d) level of theory.

Superposition of Thymidine Analogues. The initial structures of thymidine (THYDIN), **1a** (LETJEZ) and **1b** (YESMIS) were taken from the Cambridge Structural Database (CCDC ConQuest version 1.5). YESMIS is a dimer containing two conformers—monomer 1 was in a $_3T^2$ conformation (same as THYDIN) whereas monomer 2 was $_3$E. Although either monomer is adequate for this comparison, monomer 1 (Yesmis1) was used for the superposition. THYDIN was used as is, whereas the other two analogues (LETJEZ, Yesmis1) were modified so that their torsion angles χ would match that of THYDIN. The superpositions were then accomplished using the "Atoms Match" function in Accelrys' Cerius[2] (version 4.8). The number of atoms specified for superposition were chosen with the goal of maximizing the similarity between the sugar and pseudosugar rings in each case. The five atoms of the cyclopentane ring of analogue Yesmis1 (**1b**) were superposed on those of the reference compound THYDIN. The root-mean-square deviation (RMS) between the two sets of the five atoms was 0.063 871 8, implying a good match (Figure 6A). The four most planar atoms of the cyclopentane ring of the modified LETJEZ analogue (**1a**) were also superposed on those of the reference compound THYDIN as shown in Figure 6B. The RMS between the two sets of four atoms was 0.121054.

JA037929E

(34) Stott, K.; Keeler, J.; Van, Q. N.; Shaka, A. J. *J. Magn. Res.* **1997**, *125*, 302−324.